



ELSEVIER

Available online at www.sciencedirect.com

SCIENCE @ DIRECT®

Nuclear Instruments and Methods in Physics Research B 205 (2003) 178–182

NIM B
Beam Interactions
with Materials & Atomswww.elsevier.com/locate/nimb

Development of a cold HCI source for ultra-slow collisions

N. Oshima^{a,b,*}, T.M. Kojima^b, M. Niigaki^{a,b}, A. Mohri^b, K. Komaki^a,
Y. Iwai^b, Y. Yamazaki^{a,b}

^a Institute of Physics, University of Tokyo, 3-8-1 Komaba, Meguro, Tokyo 153-8902, Japan

^b Atomic Physics Laboratory, RIKEN, 2-1 Hirosawa, Wako, Saitama 351-0198, Japan

Abstract

A system consisting of a superconducting solenoid, a multi-ring trap and a slow positron source has been built to prepare a cold highly charged ion (HCI) beam, which will be applied to study interactions with solids or gases, e.g. potential energy deposition scheme during interaction of slow HCIs with a surface. An electron plasma with density more than 10^{10} cm^{-3} has already been prepared to trap positrons.

© 2003 Elsevier Science B.V. All rights reserved.

PACS: 52.55.Dy; 52.25.b; 52.27.Ep; 52.27.Jt

Keywords: Positron cooling; Slow HCI; Positron trap

1. Introduction

Interactions of slow highly charged ions (HCIs) with solid/gas have been intensively studied in the last two decades [1–10], which involves multiple electron transfer processes, the formation mechanisms of hollow atoms (ions), their evolution above and below a surface, the scheme of their potential energy deposition, etc. It is noted that the scheme on how the potential energy is deposited in a material has rarely been studied (an interesting exception can be seen, e.g., in [11]). This is in good contrast with the kinetic energy deposition scheme,

which is more or less comprehensively understood in the kinetic energy range of more than 9 digits including relativistic region. In establishing a scenario of the potential energy deposition, one needs a high quality cold HCI beam, which has not been available till now.

To produce such cold HCIs, a positron cooling technique is being developed [12–15], which is schematically drawn in Fig. 1(a)–(d). (a) A plasma consisting of $\sim 10^{10}$ electrons is prepared in a multi-ring trap (MRT) [16] which is installed in a superconducting solenoid of 5 T. The electron plasma is automatically cooled down to its environmental temperature via synchrotron radiation in the strong magnetic field. (b) A positron beam of 10^6 – $10^7 \text{ e}^+/s$ is injected into the MRT, where they are accelerated to overcome magnetic mirror effect. The positrons are first implanted into a re-moderator, and then re-emitted as slow positrons

* Corresponding author. Address: Atomic Physics Laboratory, RIKEN, 2-1 Hirosawa, Wako, Saitama 351-0198, Japan. Tel.: +81-48-467-9483; fax: +81-48-462-4644.

E-mail address: noshima@postman.riken.go.jp (N. Oshima).

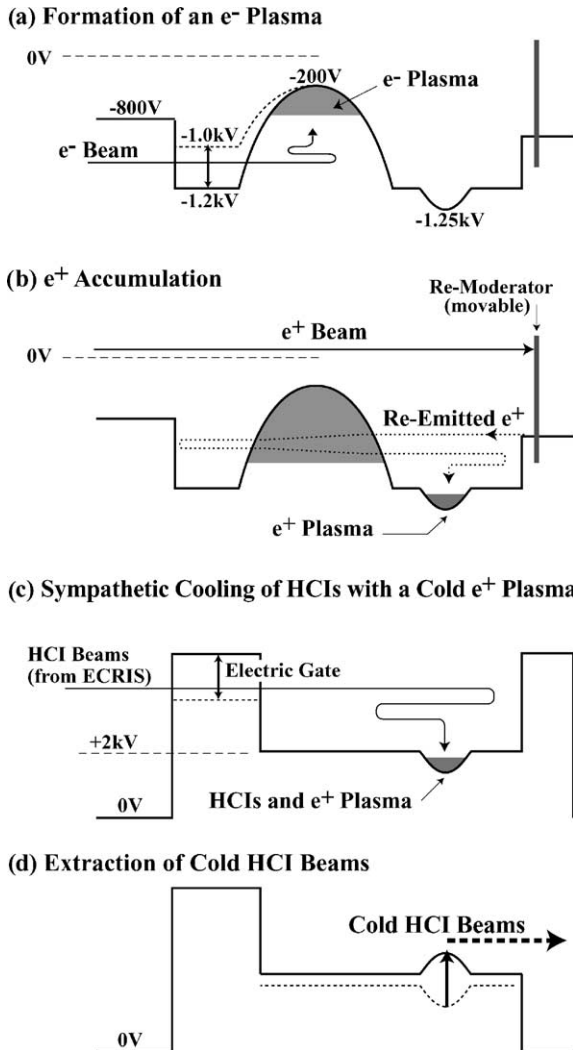


Fig. 1. (a)–(d) Schematic descriptions of the HCI trapping, cooling and extraction.

with small energy spread with a typical efficiency of 20–30% [17,18], which interact with the pre-loaded electron plasma. Both the density and length of the electron plasma are high and long enough, so that the positrons lose their energy and eventually be trapped. After trapping, they are cooled via synchrotron radiation. This stage lasts until 10^7 – 10^8 positrons are trapped. (c) 10^6 – 10^7 HCIs are injected and accumulated in the MRT, which are then cooled with the positron cloud. (d) Cold HCIs are extracted from the MRT by

ramping the potential valley as a cold HCI beam [19].

In order to realize the above scheme, we have built a system consisting of a 5 T superconducting solenoid with an ultra-high vacuum (UHV) bore tube which can be cooled down to several K, an MRT having 35 electrodes, a ^{22}Na based slow positron source with a solid Ne moderator and a beam line connected to an ECR ions source. In this paper, the design and specifications of the newly developed trap are reported.

2. Required specifications of the trap

As mentioned in the introduction, positrons are implanted into the re-moderator, to convert them as a slow monoenergetic beam (see Fig. 1(b)). A tungsten single crystal is used as the re-moderator because of its high moderation efficiency [17]. The work function of tungsten for positron is ~ 3 eV, i.e. positrons are emitted with their kinetic energy of ~ 3 eV. In order to accumulate re-moderated positrons in the MRT, the energy loss of the positrons in the electron plasma should be larger than their typical energy spread of ~ 1 eV [17]. The energy loss of positrons is proportional to the surface density of the plasma, $S = n_e L$, where n_e is the volume density of the electron plasma and L the plasma length. The required surface density for 1 eV energy loss of positrons is estimated to be $\sim 10^{12}$ cm^{-2} , in case that positrons are injected into the electron plasma with low energies ~ 5 eV [15]. Then, almost all of the re-moderated positrons will be trapped in the positron trapping well.

A harmonic potential was prepared by the MRT, which is known to store dense plasma more stably than a rectangular potential well. In our case, two harmonic potential wells are required to be formed simultaneously both for electrons and positrons.

In order to meet the above requirements, reasonable length of the MRT is considered to be 50 cm.

It takes a few seconds for cooling HCIs with positrons. During the cooling, the vacuum of the HCI trapped regions should be kept at 10^{-8} Pa or better to prevent charge transfer reaction between HCIs and residual gas atoms/molecules [13].

3. Setup of the trap

3.1. Superconducting magnet

Fig. 2 shows a schematic drawing of the superconducting solenoid, which provide a magnetic field as high as 5 T. The uniformity of the field near the center of the bore is better than 10^{-3} in the volume of $4\text{ mm } \varnothing \times 500\text{ mm}$ where plasmas are trapped. An electrochemically polished UHV vessel of $98\text{ mm } \varnothing \times 1940\text{ mm}$ is inserted in the solenoid. The vessel is thermally insulated from the beam line with two bellows so that the vessel can be baked and cooled down to several K during operation. The vessel position can be adjusted with four motor-controlled linear feedthroughs ($\pm 2\text{ mm}$) to align the vessel axis against the solenoid axis. The relative position of the vessel is monitored by four laser positioners each having position resolution of 0.01 mm .

The solenoid is equipped with two refrigerators. One is for the superconducting solenoid (NbTi) and the other is for the vessel to acquire UHV and

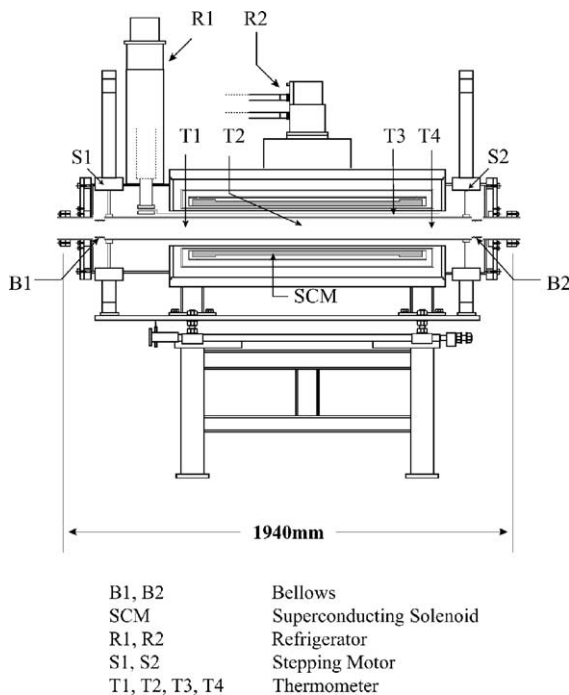


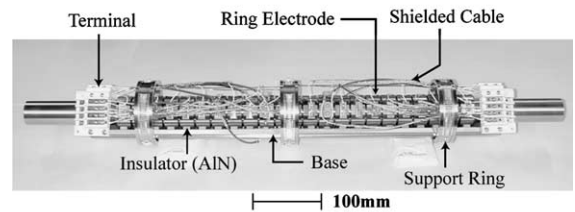
Fig. 2. A schematic drawing of the 5 T superconducting solenoid and the UHV vessel.

at the same time to prepare cold plasmas. The vessel is bakeable using pre-wired heaters. Four thermometers, which work in the strong magnetic field, are mounted around the outer wall of the vessel. The trapping region, where the MRT is installed, was cooled down to 10 K. The vacuum is monitored by two pressure gauges in the beam line near the entrance and exit of the vessel, and it is kept $2 \times 10^{-7}\text{ Pa}$ without baking. It is noted that the area around the vacuum gauges are at room temperature, i.e., the vacuum around the MRT area (10 K) should be much better than the above.

3.2. Multi-ring trap

Three electrode assemblies are prepared to form the potential distribution in the vessel, the MRT and two guiding/extraction assemblies on both sides of the MRT. Fig. 3(a) shows a photo of the MRT, which is 50 cm long and consists of 21 ring electrodes, each of which is 38 mm in inner diameter and 20 mm in length. Two of the electrodes

(a) Multi-Ring Trap (MRT)



(b) Re-Moderator Holder (movable)

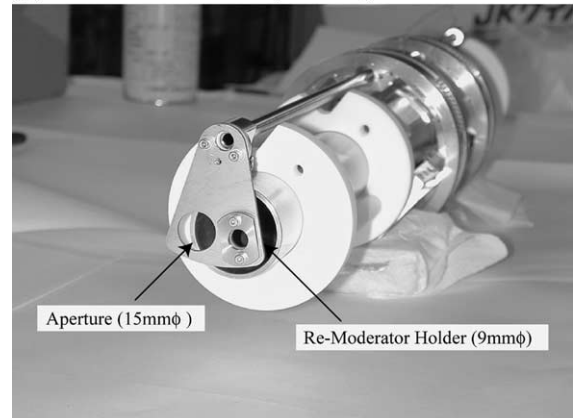


Fig. 3. Photos of (a) the MRT and (b) the re-moderator holder.

are segmented into four for detecting and driving rotational motion of plasmas. As discussed in the previous section, the MRT was designed so that it can prepare two harmonic potential regions, one for the electron plasma and the other for the positron and the HCI. On both ends, electrodes of 160 mm long are added. These electrodes are assembled on a rectangular plate. The electrodes and the rectangular plate are made of gold-plated oxygen free copper. Aluminum nitride (AlN) is adopted as the insulating material, because of its high thermal conductivity, which is essential to cool the MRT effectively by the cold vessel still keeping electrical insulation. Three support rings with multi-contact bands on their outer surfaces allow effective thermal contact between the MRT and the vessel. The bands also absorb mechanical stress induced by heat cycles.

The positron re-moderator made of a tungsten single crystal is positioned at an end of the MRT. As is shown in Fig. 3(b), the re-moderator is on the movable holder so that it is removable when particles are extracted downstream of the MRT.

4. Electron plasma

A 26 mm \varnothing fluorescence screen which is used also as a Faraday cup is located at ~ 1 m downstream from the MRT, where the magnetic field is ~ 0.05 T, i.e. the radial distribution observed here is 10 times wider than that in the MRT. A thin fluorescent material is applied on an ITO conducting glass and coated with a 0.025 μm aluminum layer to avoid charging up. The total number of electrons in the MRT is determined by the charge detected at the re-moderator or at the fluorescence screen during extraction. The diameter of the plasma in the MRT is determined by observing the image on the fluorescence screen with a CCD camera.

Electrons from an electron gun 25 mm off-axis from the magnet axis are injected into the trap adjusting the injection position with an $E \times B$ field.

Fig. 4 shows the number of electrons trapped in the MRT as a function of injection time when the incident electron beam is 1 μA . The inset shows the CCD image of the electron plasma (the total

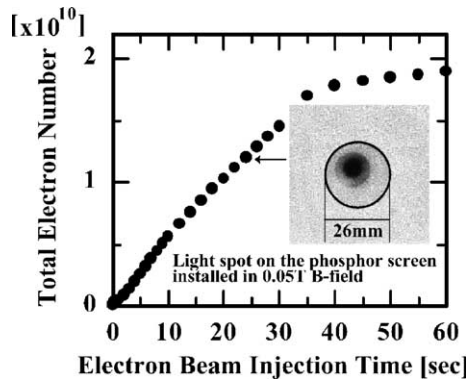


Fig. 4. The number of trapped electrons as a function of the electron injection time for an electron beam of 1 μA . The inset shows the CCD image of the extracted plasma at $B = 0.05$ T.

number of electrons is 1.2×10^{10}) trapped for 10 s, which tells that the plasma diameter is ~ 1 mm. Assuming that the plasma has a spheroidal shape, the surface density of the plasma is evaluated [20] to be $\sim 2.3 \times 10^{12} \text{ cm}^{-2}$ ($n_e = 7.4 \times 10^{10} \text{ cm}^{-3}$, $L = 31$ cm), which meets the requirements described in Section 2.

Acknowledgements

The authors are grateful to H. Higaki, T. Kambara, Y. Kanai, Y. Nakai, H. Oyama and M. Wada for their helpful suggestions, to S. Letout, A. Sakai and H. Sato for help in the apparatus development.

References

- [1] J.P. Briand, L. de Billy, P. Charles, S. Essabaa, P. Briand, R. Geller, J.P. Desclaux, S. Bliman, C. Ristori, Phys. Rev. Lett. 65 (1990) 159.
- [2] J. Burgdörfer, P. Lerner, F.W. Meyer, Phys. Rev. A 44 (1991) 5674.
- [3] H. Kurz, K. Töglhofer, HP. Winter, F. Aumayr, R. Mann, Phys. Rev. Lett. 69 (1992) 1140.
- [4] J. Das, R. Morgenstern, Phys. Rev. A 47 (1993) R755.
- [5] F.W. Meyer, C.C. Havener, P.A. Zeijlmans van Emmichoven, Phys. Rev. A 48 (1993) 4476.
- [6] M. Grether, A. Spieler, R. Köhrbrück, N. Stolterfoht, Phys. Rev. A 52 (1995) 426.
- [7] N. Kakutani, T. Azuma, Y. Yamazaki, K. Komaki, K. Kuroki, Jpn. J. Appl. Phys. 34 (1995) L580.

- [8] S. Ninomiya, Y. Yamazaki, F. Koike, H. Masuda, T. Azuma, K. Komaki, M. Sekiguchi, *Phys. Rev. Lett.* 78 (1997) 4557.
- [9] A. Arnau, F. Aumayr, P.M. Echenique, M. Grether, W. Heiland, J. Limburg, R. Morgenstern, P. Roncin, S. Schippers, R. Schuch, et al., *Surf. Sci. Rep.* 27 (1997) 113.
- [10] J.D. Gillaspay, *J. Phys. B* 34 (2001) R93.
- [11] T. Schenkel, A.V. Barnes, T.R. Niedermayr, M. Hattass, M.W. Newman, G.A. Machicoane, J.W. McDonald, A.V. Hamza, D.H. Schneider, *Phys. Rev. Lett.* 83 (1999) 4273.
- [12] N. Oshima, T.M. Kojima, D. Dumitriu, A. Mohri, H. Oyama, T. Kambara, Y. Kanai, Y. Nakai, M. Wada, Y. Yamazaki, *RIKEN Rev.* 31 (2000) 65.
- [13] T.M. Kojima, N. Oshima, D. Dumitriu, H. Oyama, A. Mohri, Y. Yamazaki, *RIKEN Rev.* 31 (2000) 70.
- [14] N. Oshima, T.M. Kojima, A. Mohri, M. Niigaki, T. Kambara, Y. Kanai, Y. Nakai, H. Oyama, M. Wada, Y. Yamazaki, *ICPEAC Abstr.* 22 (2001) 681.
- [15] A. Mohri, T.M. Kojima, N. Oshima, M. Niigaki, Y. Yamazaki, in: F. Anderegge et al. (Eds.), *AIP Conference Proceedings 606*, American Institute of Physics, New York, 2002, p. 634.
- [16] A. Mohri, H. Higaki, H. Tanaka, Y. Yamazawa, M. Aoyagi, T. Yuyama, T. Michishita, *Jpn. J. Appl. Phys.* 37 (1998) 664.
- [17] P.J. Schultz, K.G. Lynn, *Rev. Mod. Phys.* 60 (1988) 701.
- [18] R. Suzuki, T. Ohdaira, A. Uedono, Y.K. Cho, S. Yoshida, Y. Ishida, T. Ohshima, H. Itoh, M. Chiwaki, T. Mikado, et al., *Jpn. J. Appl. Phys.* 37 (1998) 4636.
- [19] M. Niigaki, N. Oshima, T.M. Kojima, Y. Yamazaki, *ICPEAC Abstr.* 22 (2001) 689.
- [20] D.H.E. Dubin, T.M. O’Neil, *Rev. Mod. Phys.* 71 (1999) 87.